Pure & Appl. Chem., Vol. 61, No. 5, pp. 795–804, 1989.
Printed in Great Britain.

Structure and reactivity of rhodium(II) complexes

Florian P. Pruchnik

Institute of Chemistry, University of Wrocław, 14 Joliot Curie Street, 50-383 Wrocław, Poland

Abstract - Complexes containing the Rh_2^{4+} core are extensively investigated both from the theoretical and practical points of view. Properties, reactivity and electronic structure of complexes with Rh_2^{4+}, Rh_2^{3+} and Rh_2^{5+}: $[Rh_2X_2(OOCR)_2(N\text{-}N)_2]^n$ and $[Rh_2(OOCR)_4]^n$ (n=1,0,-1) are discussed. The calculations confirmed the reasonable stability of $[Rh_2(OOCR)_4]^-$ compounds. The effect of axial and equatorial ligands on electronic structure of complexes and on stability of the Rh-Rh bond was investigated. Assignment of the ν(Rh-Rh) stretching frequency is discussed on the ground of the normal coordinate analysis and potential energy distribution calculations. The redox reactions of complexes under study were examined. Their catalytic properties in reduction reactions of olefins and ketones were investigated. The mechanism of formation of catalytically active complexes is discussed.

INTRODUCTION

The chemistry of rhodium is among the most diverse of all the transition metals and is being vigorously investigated at the present time. The most common oxidation states of rhodium are +1 and +3. The monomeric rhodium(II) compounds are unstable, contrary to the dimeric rhodium complexes containing the rhodium-rhodium bond. Among them the most important are the $Rh_2(OOCR)_4$ carboxylates and their analogs. The studies of these compounds led to the creation of chemistry of the new oxidation states of the other platinum metals, that is, Ru(I), Os(I), Pt(III). The development of chemistry of the rhodium(II) dimers observed recently, is due to the interest in the theory of the electronic structure of clusters with the single metal-metal bond, their spectroscopic properties and reactivity as well as their possible practical applications (ref. 1-3). Binuclear rhodium(II) complexes are effective catalysts in reduction of olefins and ketones and in oxidation of alkenes and alkyl-aromatic hydrocarbons; they also catalyze the reactions of the diazo compounds with RXH (X=O,S,NH) and with olefins to produce cyclopropane derivatives. They are the catalysts of silylation, of the photocatalytic decomposition of water, etc. The rhodium(II) carboxylates $Rh_2(OOCR)_4$ are also the most promising antitumor compounds.

The majority of the rhodium(II) complexes contains bridge ligands, most frequently the carboxylate ligands $[Rh_2(\mu\text{-}OOCR)_4L_2]$, where L is the Lewis base. The compounds containing either lower number of bridges, e.g.: $[Rh_2(OAc)_3(py)_4]CFSO_3$, (ref. 4), $[Rh_2X_2(OOCR)_2(chel)_2]$ (X=Cl, Br, I,; R = H, Me, $CH(OH)C_6H_5$; chel=2,2-bipyridine (bpy), 1,10-phenanthroline (phen) and its derivatives) (ref. 5-9), or not containing bridge ligands, e.g.: $[Rh_2(dmg)_4]$ (ref. 1-3), $[Rh_2L_{10}]^{4+}$ (ref. 4,11) are also known. The Rh-Rh bond length depends upon the number and properties of the bridge ligands. For complexes with 4 bridge ligands the value of bond length lies in the limits from 235.9 pm for $Rh_2(mhp)_4$ (mhp = 2-oxy-6-methylpyridinate) to 249 pm for $[Rh_2(H_2PO_4)_4(H_2O)_2]$. In the complexes with two RCOO bridges the Rh-Rh distance is 255-262 pm (ref. 9,12,13); in the bridge-free compounds it changes from 262.5 pm for $Rh_2(C_{22}H_{22}N_4)_2 \cdot 3C_6H_6$ to 293.6 pm for $[Rh_2(dmg)_4(PPh_3)_2] \cdot C_3H_7OH \cdot H_2O$.

The Rh-Rh bond in all rhodium(II) dimers is now assumed to be single, although the distance between the rhodium atoms was found to vary within very broad limits. This was confirmed by the extended Hückel (ref.14), SCF-Xα-SW (ref. 15) and ab initio (ref. 16,17) calculations, which gave the $\sigma^2\pi^4\delta^2$

$\delta^{*2}\pi^{*4}$, $\sigma^2\pi^4\delta^2\pi^{*4}\delta^{*2}$ and $\pi^4\delta^2\pi^{*4}\delta^{*2}\pi^2$ electronic configurations. The results indicate that the electronic structure depends on the nature of not only axial, but also of other ligands. Somewhat doubtful is also the assignment of the $\nu(Rh_2)$ stretching vibration, which was estimated to be about 300 cm^{-1} (ref.18) or as 150-180 cm^{-1} (ref.19,20).

THE STRUCTURE OF $Rh_2X_2(OOCR)_2(N-N)_2$ COMPLEXES

In order to gain some additional information about the properties, structure and reactivity of the Rh(II) complexes, we have studied the $Rh_2X_2(OOCR)_2(N-N)_2$ dimers (1 : X = Cl, R=H, N-N=bpy; 2: Cl, H, phen; 3: Br, H, phen; 4: Cl, Me, bpy; 5: Br, Me, bpy; 6: I, Me, bpy; 7: Cl, Me, phen; 8: Br, Me, phen; 9: I, Me phen; 10: Cl, CH(OH)Ph, bpy; 11: Br, CH(OH)Ph, bpy; 12: I, CH(OH)Ph, bpy; 13: Cl, CH(OH)Ph, phen; 14: Br, CH(OH)Ph, phen; 15: I, CH(OH)Ph, phen) and $Rh_2(OOCR)_4(H_2O)_2$ (16: R=H; 17: R=Me; 18: R=CH(OH)Ph) (ref.5-10). The exchange of ligands, both axial and equatorial ones, allows the elucidation of the relation between the properties of complexes and the nature of ligands and the comparison of the properties of complexes under the study with those of $Rh_2(OOCR)_4$ complexes. The structure of complexes with two carboxylato ligands is shown in Fig.1. The Rh-Rh distance for $[Rh_2Cl_2(OOCH)_2(phen)_2]$ (ref.5,9), $[Rh_2Cl_2(OOCH)_2(bpy)_2]\cdot 4H_2O$ (ref.9,21), $[Rh_2Cl_2(OOCCH(OH)C_6H_5)_2(bpy)_2]\cdot 6H_2O$ (ref.22), $[Rh_2(OAc)_2(phen)_2(mid)_2](ClO_4)_2$ (mid = N-methylimidazole) (ref.13), $[Rh_2(OAc)_2(3,4,7,8\text{-}Me_4phen)_2(mid)_2](ClO_4)_2$ (ref. 13) and $[Rh_2(OAc)_2(dmg)_2(PPh_3)_2]\cdot H_2O$ (see ref. 1-3) are equal to 257.6 pm, 257.8 pm, 257.0 pm, 255.6 pm 256.4 pm and 261.8 pm, respectively.

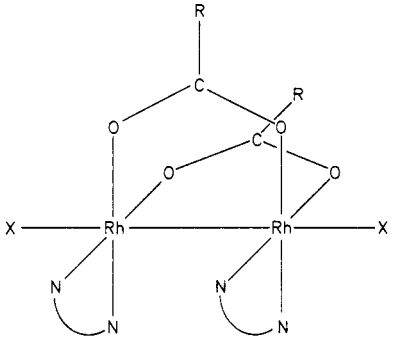

Fig.1. Structure of the $[Rh_2X_2(OOCR)_2(N-N)_2]$ complexes.

The Rh-O distance are somewhat longer (up to 4 pm) than in $[Rh_2(OOCR)_4]$ complexes, while the Rh-Cl distance is by 7-9 pm shorter than in the $[Rh_2(OOCMe)_4Cl_2]^{2-}$ dimer. The Rh-Rh bond lengths in complexes with two bridges exceed by ca. 17 pm those in the appropriate $[Rh_2(OOCR)_4]$ tetracarboxylates. In order to elucidate the electronic structure of $[Rh_2X_2(OOCR)_2(N-N)_2]$ (N-N=bpy, phen) complexes, and to compare it with the structure of $Rh_2(OOCR)_4$ compounds, we have performed the calculations of the electronic structure of complexes 16, $[Rh_2X_2(OOCH)_2(HN=CH-CH=NH)_2]$, (X = Cl, Br, I) and $[Rh_2(OOCH)_2(HN=CH-CH=NH)_2L_2]^{2+}$ (L = H_2O, NH_3, PH_3, AsH_3) by the Fenske-Hall method (ref.23). For diaquatetraformatodirhodium(II) the following molecular orbitals sequence was achieved: $\sigma^2\pi^4\delta^2\delta^{*2}\pi^{*4}$ (ref. 24), that

TABLE 1. Some upper valence energy levels (eV) and charge distributions.

$Rh_2(OOCH)_4(H_2O)_2$				$Rh_2Cl_2(OOCH)_2(C_2N_2H_4)_2$				$Rh_2Br_2(OOCH)_2(C_2N_2H_4)_2$			
D_{4h} level	energy	% charge 2Rh	ligands	C_{2v} level	energy	% charge 2Rh	ligands	C_{2v} level	energy	% charge 2Rh	ligands
$5a_{1g}$ σ	-11.25	77	23	$13a_1$ σ	-13.96	57	43	$13a_1$ σ	-13.04	64	36
$6e_u$ π	-10.73	81	19	$14a_1$ π	-12.84	54	46	$14a_1$ π	-12.54	56	44
$2b_{2g}$ δ	- 9.96	91	9	$11b_2$ π	-12.33	71	29	$11b_2$ π	-12.00	75	25
$2b_{1u}$ δ^*	- 7.80	75	25	$13b_1$ π^*	-11.29	45	55	$13b_1$ π^*	-10.86	63	37
$5e_g$ π^*	- 7.76	90	10	$15a_1$ δ	-10.61	75	25	$15a_1$ δ	-10.43	76	24
$4a_{2u}$ σ^*	- 2.39	82	18	$15b_1$ δ^*	- 9.33	68	32	$10a_2$ π^*	-10.31	46	54
$4b_{2u}$ σ^*RHO	0.36	68	32	$11a_2$ π^*	- 9.16	50	50	$15b_1$ δ^*	- 9.10	62	38
$5b_{1u}$ σ^*RHO	0.48	64	36	$18a_1$ π^*NC	- 7.33	17	83	$18a_1$ π^*NC	- 7.03	15	85
				$16b_1$ π^*NC	- 6.51	24	76	$16b_1$ π^*NC	- 6.29	24	76
				$17b_1$ σ^*	- 2.85	63	37	$17b_1$ σ^*	- 2.97	60	40

is the same as that obtained by the extended Hückel (ref. 14) and ab initio SCF/CI (ref. 17) methods. The obtained energy values of δ^* and π^* orbitals are only slightly different, like in the case of the other methods (ref.14, 15,17). The 1,4-diaza-1,3-butadiene molecule, like the 2,2'-bipyridine one, contains the conjugated system of double bonds N=C-C=N, and thus the results of calculations for complexes with HN=CH-CH=NH and 2,2-bipyridine should be similar. Substitution of two formato ligands by two HN=CH-CH=NH molecules removes the degeneracy of π(Rh-Rh) and π^*(Rh-Rh) orbitals. Between the π^* and σ^* orbitals of the Rh_2^{4+} core there are the empty π^* orbitals of the diene ligand, with considerable contribution of d_π orbitals of rhodium. This is indicative for the π-acceptor properties of 1,4-diaza-1,3-butadiene. The bonding σ, π, δ orbitals, as well as the antibonding σ^*, π^*, δ^* orbitals in the $[Rh_2X_2(OOCH)_2(HN=CH-CH=NH)_2]$ complexes contain considerable contributions of ligand orbitals, as compared with $[Rh_2(OOCH)_4(H_2O)_2]$ (Table 1). Also the contribution of d orbitals of rhodium in Rh-ligand orbitals grows. It is especially strong in the case of σ, π, σ^* and π^* orbitals. Such a situation is due mainly to the interaction between the Rh_2^{4+} core orbitals and HN=CH-CH=NH orbitals as well as with the axial ligand orbitals (Cl, Br, I). This is responsible for the lowering of energy of σ, π and π^* orbitals, but, since the greater contribution of ligand orbitals it changes the character of Rh-Rh bond, and, finally, leads to the weakening of the bond between central atoms. The contribution of σ^*(Rh-Rh)($17b_1$) orbital to the σ(Rh-X)($12b_1$) orbital grows in the order Cl< Br< I. This is consistent with the electronegativity decrease of halogens in the same direction. It means, that weakest becomes the σ(Rh-Cl) bond, under the effect of the trans σ(Rh-Rh) bond. As the result of interaction with the empty π^*(CN) orbitals, the π($14a_1$) and π^* ($13b_1$) orbitals of the Rh_2^{4+} core, deriving from π($5e_u$) and π^*($5e_g$) orbitals of the $[Rh_2(OOCH)_4(H_2O)_2]$ complex, respectively, are stabilized. This stabilization is additionally increased by interaction with p orbitals of the halide ligands. In the cationic $[Rh_2(OOCH)_2(HN=CH-CH=NH)_2L_2]^{2+}$ complexes (L = H_2O, NH_3, PH_3, AsH_3), the degeneracy of the π and π^* of Rh_2^{4+} core is also removed and the electron density is shifted towards the HN=CH-CH=NH ligands; in this case, however the mixing of the ligands orbitals with the Rh_2^{4+} core orbitals is smaller. The mutual interaction of the axial ligands with rhodium orbitals is unusually effective in the case of PH_3 and AsH_3 (Fig. 2). For

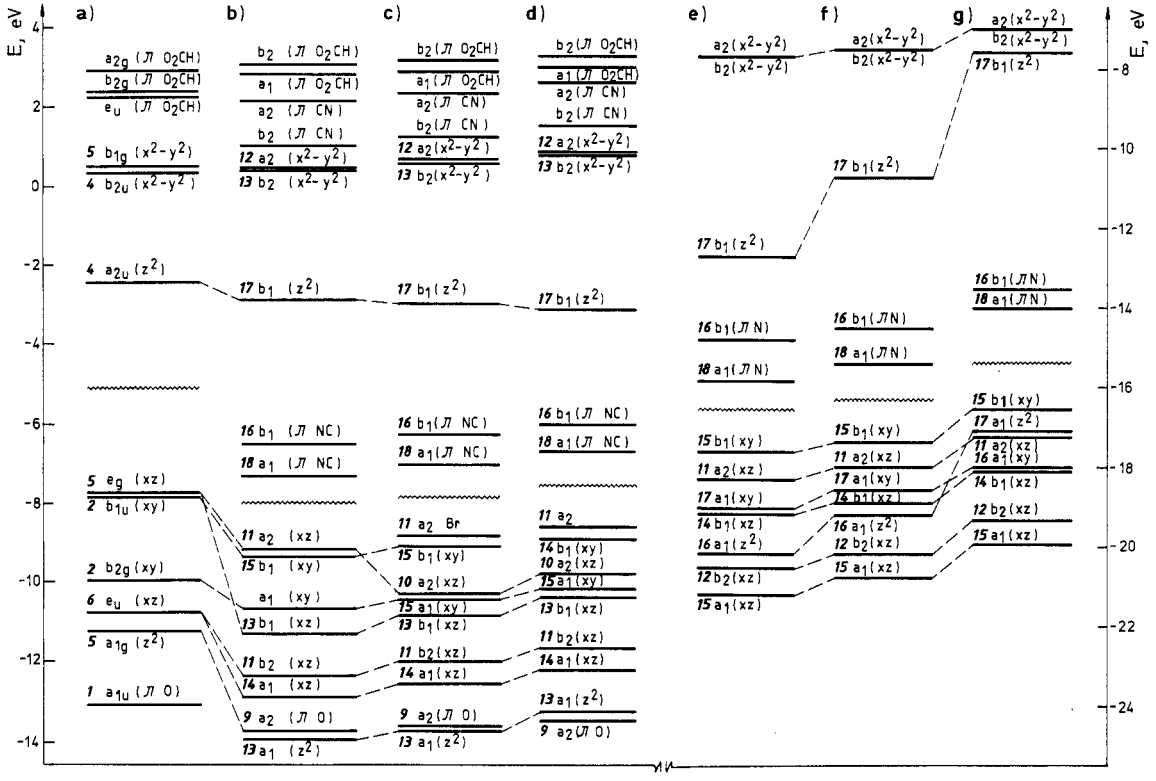

Fig. 2. Most important energy levels of $[Rh_2(OOCH)_4(H_2O)_2]$-a, $[Rh_2X_2(OOCH)_2(HN=CH-CH=NH)_2]$ (X = Cl - b, Br - c, I - d) and $[Rh_2(OOCH_2)(HN=CH-CH=NH)_2L_2]^{2+}$ (L = H_2O - e, NH_3 - f, PH_3 - g).

complexes with H_2O and NH_3 the sequence of the molecular orbitals is the following $\pi_1^2\pi_2^2\sigma^2\pi_1^{*2}\delta^2\pi_2^{*2}\delta^{*2}\pi_1^*(NC)\pi_2^*(NC)\sigma^*$. Because of the increase of the σ-donor properties of axial ligands in the order $H_2O < NH_3 < PH_3 < AsH_3$, the mixing of the orbitals of axial ligands and those of 1,4-diaza-1,3-butadiene with d_{z^2} orbitals is greater. This leads because of considerable destabilization of the σ and σ^* orbitals of Rh_2^{4+} core to the following orbital order for complexes with PH_3 and AsH_3: $\pi_1^2\pi_2^2\pi_1^{*2}\delta^2\pi_2^{*2}\sigma^2\delta^{*2}\pi_1^*(NC)\pi_2^*(NC)\sigma^*$. These calculations supply the explanation of the greater Rh-Rh bond length in complexes with phosphines and arsines as axial ligands, as compared with complexes containing the oxygen and nitrogen axial ligands. Calculations performed for Rh_2^{4+} complexes, namely, for $[Rh_2(OOCH)_4(H_2O)_2]$ and $[Rh_2X_2(OOCH)_2(HN{=}CH{-}CH{=}NH)_2]$ suggest, that these compounds should be rather stable, although they should show very strong reduction properties. Electron configurations here are the following: $\sigma^2\pi^4\delta^2\pi^{*4}\delta^{*2}\sigma^{*1}$ and $\sigma^2\pi_1^2\pi_2^2\pi_1^{*2}\delta^2\pi_2^{*2}\delta^{*2}\pi_1^*(NC)\pi_2^*(NC)\sigma^*$, respectively. The results of calculations were confirmed by the electronic absorption spectra (ref. 6,8) (Table 2). Like in the case of the tetracarboxylato complexes, the spectra of $Rh_2X_2(OOCR)_2(N{-}N)_2$ show at 18000 cm^{-1} a weak band ($\varepsilon \sim 200 - 400$) assigned to the $^2\pi^*(Rh_2) \rightarrow {}^2\sigma^*(Rh_2{=}O)$ transition (ref.19); according to our expectations, its energy exceeds that of the transition in $Rh_2(OOCR)_4$ since the $\pi^*(Rh_2)$ orbitals are stabilized because of interaction with π^* orbitals of the nitrogen ligands. At about 22000 cm^{-1} an intensive band is observed, which could be assigned to the $\sigma(Rh_2) \rightarrow \pi^*(N{=}C)$ transition, that is to the MLCT transition, i.e. to the electron transfer from rhodium to the empty π^* orbitals of the nitrogen ligands (bpy or phen). Again, as in $[Rh_2(OOCR)_4X_2]^{-2}$ complexes (ref. 19), the ligand to metal charge transfer bands $\sigma(Rh{-}X) \rightarrow \sigma^*(Rh_2)$ at 37000, 32000 and 25000 cm^{-1} were discovered for the chloride, bromide and iodide complexes, respectively (ref. 6,8).

TABLE 2. Electronic spectra of $[Rh_2X_2(OOCR)_2(N{-}N)_2]$ complexes.

Complex Solvent	Bands μm^{-1} ($\varepsilon \cdot 10^{-2}$, $M^{-1}cm^{-1}$)
1, H_2O	1.79(2.20), 2.42(21), 2.86(35), 3.08(68), 3.30(181), 3.77(345), 3.92(366)
2, H_2O	1.775(2.30), 2.50(26), 2.78(40), 3.74(367), 4.03(397), 4.48(428)
7, H_2O	1.76(2.60), 2.45(27.5), 2.76(45), 3.71(350), 3.97(466), 4.44(466)
10, EtOH	1.80(4.00), 2.30(30), 2.65(53), 3.23(230), 3.66(394)
11, MeOH	1.80(3.30), 2.33(33), 2.60(55), 3.03(166), 3.24(219), 3.66(320)
12, MeOH	1.83(7.50), 2.21(67), 2.50(144), 2.79(134), 3.25(126), 3.58(2.30) 3.79(207), 3.86(198)
13, EtOH	1.80(3.70), 2.30(32), 2.63(54), 3.29(188), 3.55(275), 3.68(319), 3.86(396).
14, MeOH	1.80(2.00), 2.31(25), 2.62(42), 3.15(117), 3.79(192), 3.89(265)
15, MeOH	1.81(4.20), 2.22(50), 2.55(92), 2.80(97), 3.31(102), 3.88(278)

REACTIVITY

Calculations for $[Rh_2X_2(OOCH)_2(HN{=}CH{-}CH{=}NH)_2]$ and $[Rh_2(OOCH)_4(H_2O)_2]$ suggest that during the reduction of the former, the unpaired electron should be located on the $\pi^*(N{=}C)$ orbital of 1,4-diaza-1,3-butadiene, whereas in the latter on the antibonding $\sigma^*(Rh_2)$ orbital, with only minor contribution from $\sigma^*(Rh{-}L)$. The studies of reduction of 1,2,10,16,17, and 18 complexes in polar solvents (CD_3OD, CD_3COCD_3 and $DCON(CD_3)_2$ by radiolysis using ^{60}Co γ-rays (ref. 27) revealed, that their reactions with the reducing radicals formed at irradiation at 77 K, produced the complexes $[Rh_2(OOCR)_4(H_2O)_{2-n}(solv)_n]^{-}$ and $[Rh_2X_{2-n}(OOCR)_2(N{-}N)_2(solv)_n]^{(n-1)+}$, because owing to the strong trans-influence of the Rh-Rh bond, the axial ligands are easily substituted by solvent molecules or by other ligands. Monomers $[Rh(OOCR)_2L_m]$ (R = H, CH(OH)Ph) and $[RhX_m(OOCR)_{2-m}L_2]^{(1-m)+}$ are also formed. In the case of rhodium(II) acetate, at the liquid nitrogen temperature only $[Rh_2(OAc)_4]$ was formed (ref. 27), in which an electron is located on the σ^* orbital and both rhodium atoms are equivalent. Under annealing of the frozen solutions at first only several bridge bondings are broken; next follows the formation of a dimer with an unpaired electron localized on one of the rhodium atoms, and finally, the dissociation of the compound to the Rh(II) and Rh(I) complexes.

In the case of the Rh(II) formate and mandalate the irradiation is followed not only by the reduction of complexes to $[Rh_2(OOCR)_4]^-$ but also their dissociation, with formation of Rh(II) monomers, because of the break of the Rh-Rh bonding.

$$2[Rh_2(OOCR)_4] \xrightarrow{77\ K} [Rh_2(OOCR)_4]^- + 2[Rh(OOCR)_2]$$

R=H $g_\perp = 2.230$, $g_\parallel = 2.00$ $g_1 = 2.532$, $g_2 = 2.064$, $g_3 = 2.00$

R=CH(OH)Ph $g_\perp = 2.241$, $g_\parallel = 2.00$ $g_1 = 2.512$, $g_2 = 2.046$, $g_3 = 2.00$

$$[Rh_2(\mu\text{-}OOCR)_2(OOCR)_2]^- \xrightarrow{130\ K} [(RCOO)Rh(\mu\text{-}OOCR)Rh(OOCR)_2]^- \xrightarrow{150\ K} \quad (1)$$

R=H $g_x = 2.304$, $g_y = 2.230$

$$[Rh(OOCR)_2] + [Rh(OOCR)_2]^-$$

Paramagnetic Rh_2^{3+} and mononuclear Rh(II) compounds are stable only in frozen solutions. The melting of solutions results in their immediate decomposition. Electrochemical reduction of 18 in methanol is an irreversible process, as it was demonstrated by cyclic voltammetry measurements (ref. 10). The formed Rh(II)-Rh(I) complex most likely reacts immediately with the solvent. Electro reduction gives two reduction peaks, while it does not show the coupled oxida tion peaks on the backward sweep. If the cathodic sweep direction is reversed at any point beyond the first reduction peak, the current returns through the cathodic (or inverted) peak at approximately the same potential as the for- ward peak. A reasonable explanation for the inverted current of the reverse cyclic sweep is that the adsorbed 18 complex is either desorbed or reoriented at potentials beyond the reduction peak, and then readsorbed and reduced when the potential is made more positive again. The inverted peak may also be at- tributed to amalgam formation of the reduced complex with the mercury drop electrode. The compound Rh(II)Rh(I) is much more stable in the aprotic sol- vent, DMF. The cyclic voltammetry studies revealed its quasi-reversible reduc tion on the mercury drop electrode to $\underline{18}^-$, the half-wave potential is -1.95 V vs .SCE (ref. 31). Quasi-reversible reduction points out to the probable considerable structure changes of the $\underline{18}^-$ complex. The magnetic moment of electrochemically generated $\underline{18}^-$ complex, determined by the Evans method, is at 302 K equal to 1.72 B.M. The ESR spectrum of $\underline{18}^-$ in DMF consists of one broad signal at g = 2.40. The g_1 value for the $\underline{18}^-$ complex obtained after radiolysis of 18 in DMF using ^{60}Co γ-rays at 77 K is equal to 2.241. The difference is most likely due to the different complex structure. In the $\underline{18}^-$ compound obtained at 77 K the electron is localized on both rhodium atoms. It was suggested that annealing of $\underline{17}^-$ at higher temperatures (130 K) caused splitting of acetato bridges and formation of $[MeCOORh(\mu\text{-}OOCMe)Rh(OOCMe)_2]^-$ complex with $g_x = 2.32$ and $g_y = 2.25$ (ref. 27). In the DMF solution the $\underline{18}^-$ complex is more stable, but its structure is most likely similar to that pro- posed for an acetate, i.e. with one or two mandalato bridges and with an elec tron localized mainly on one of the rhodium atoms. The 18 complex in DMF solu tion is reversibly oxidated at SMDE to the $\underline{18}^+$ complex ($E_{1/2}$ = 0.175 V vs SCE). Reduction of 1, 2 and 10 by radiolysis using ^{60}Co γ-rays in CD_3OD and $DCON(CD_3)_2$ solutions at 77K leads to the formation of axially symmetric anio- nic complexes $\underline{1}^-$, $\underline{2}^-$ and $\underline{10}^-$ with $g_\perp$ values 2.200, 2.200 and 2.185, respec- tively. In these complexes the electron is located primarily in a combination of d_{z^2} orbitals. This was confirmed by the presence of a poorly defined trip- let in $\underline{10}^-$ in DMF after annealing to ca. 100 K (A value is ca. 0.4 mT). Heat- ing of samples in the range 77 - 140 K yields the new compounds with $g_\perp$ valu- es 2.244, 2.244 and 2.230, respectively. They are, most likely, dinuclear complexes with nonequivalent rhodium atoms. In the case of $\underline{1}^-$ the intensity ratio of signals with $g_\perp$ = 2.200 and $g_\perp$ =2.244 declines linearly in the tempe rature range 77 - 130 K. The content of the complex with the electron located on both rhodium atoms decreased to zero at 140 K. The ESR spectra of $\underline{1}^-$, $\underline{2}^-$, $\underline{10}^-$, $\underline{16}^-$, $\underline{18}^-$ (ref. 26) and $\underline{17}^-$ (ref. 27) only slightly depend on the nature of the solvent. The g values for these complexes in CD_3OD, $DCON(CD_3)_2$ are the same. This is consistent with relatively low sensitivity of half-wave poten- tials for reduction of tetrakis(N,N'-di-p-tolylformamidato)dirhodium(II) to the Gutmann donor number of solvent (ref. 28). Continuous heating of a solu- tion up to the room temperature allowed the observation of the paramagnetic compounds with g = 2.00. We believe that it is a complex with the unpaired electron located in the orbital of 2,2'-bipyridine ligand. The confirmation of such supposition is the formation of the analogous compound under electro- lytic reduction of 1 in DMF as a solvent. These results were next supported

by calculations of electronic structure of $[Rh_2X_2(OOCH)_2(HN{=}CH{-}CH{=}NH)_2]$, which revealed that the LUMO orbital was the $\pi^*(HN{=}CH{-}CH{=}NH)_2$ orbital.

VIBRATIONAL SPECTRA

Rhodium(II) complexes $[Rh_2(OOCR)_4L_2]$ and $Rh_2X_2(OOCR)_2(N{-}N)_2$ are typical examples of a strong metal-metal single bond. One of the most fundamental indicators of bond strength is the stretching frequency and derived force constant of the M-M bond. Rhodium(II) complexes with two carboxylate bridges are attractive objects for investigations, because the Rh-Rh distance here exceeds by about 17 pm that in $Rh_2(OOCR)_4$, which should facilitate the interpretation of the results and comparison between these two groups of compounds. The normal coordinate analysis (NCA) and potential energy distribution (PED) calculations were performed for the $Rh_2O_4N_4Cl_2$ dimeric molecular system of the C_{2v} symmetry which is common for complexes under investigations (ref. 32). The calculations show a high degree of coupling inside the $Rh_2O_4N_4Cl_2$ core. The strongest mixing occurs between ν(Rh-Rh) and ν(Rh-X) modes of the linear X-Rh-Rh-X skeleton. In Table 3 the variations of the PED and frequencies as a function of K_{RhRh} values for selected symmetry coordinates are given. These data revealed that the ν_3 and $\nu_4(A_1)$ frequencies are the result of the ν(Rh-Rh) and ν(Rh-Cl) interaction. For the strong Rh-Rh bonds (K_{Rh-Rh}=1.85mdyne A^{-1}) the contribution of the Rh-Rh stretch is greater, while in the case of the K_{Rh-Rh} values lower than ca. 1.15 mdyne A^{-1} the contribution of Rh-Cl stretch is predominant. The calculated ν_3 and ν_4 values change within the limits 293 - 230 cm^{-1}. A reverse situation is found for ν_6 and ν_7 frequencies. In the case of the strong rhodium-rhodium bonds the contribution of Rh-Cl stretch is dominant and for the low K_{RhRh} values (1.35 mdyne A^{-1}) the Rh-Rh stretch is predominant. These frequencies are equal to 180-150 cm^{-1}. From these calculations it follows, that in the dimeric rhodium(II) complexes none of the observed frequencies was the pure rhodium-rhodium stretch, whose contribution of the ν_3 and ν_4 and ν_6 and ν_7 frequencies is different in dependence on the Rh-Rh distance, nature of axial ligands, and, to some extend, of equatorial ligands. All these factors determine the ν(Rh-Rh) energy. The ν(Rh-Rh) frequency in the case of strong Rh-Rh bonds should be assigned to the band in the range 260 - 300 cm^{-1}, while in the case of weak Rh-Rh bonds to the band in the region 110-170 cm^{-1} (Table 3).

TABLE 3. Variation of PED and wavenumbers with K_{RhRh} for selected symmetry coordinates.

ν in cm^{-1} PED in %	K_{RhRh}=1.85	1.55	1.25	0.95	0.65	0.35
$\nu_3 \rightarrow \nu_4(A_1)$	ν_3:293.38	278.68	264.46	ν_4:251.23	239.75	230.59
S_3 ν(RhCl)	30.07	36.54	45.21	56.27	68.91	80.98
S_4 ν(RhRh)	62.40	55.98	47.71	37.52	26.25	15.74
$S_8+S_9+S_{10}+S_{11}$ out-of-plane bending	7.39	7.38	7.03	6.19	4.84	3.26
$\nu_6 \rightarrow \nu_7(A_1)$	ν_6:180.49	176.44	170.42	162.20	150.54	ν_7:137.49
S_3 ν(RhCl)	53.61	43.36	30.55	16.48	4.61	0.01
S_4 ν(RhRh)	28.69	34.74	41.41	46.32	43.63	19.29
$S_8+S_9+S_{10}+S_{11}$	16.82	21.00	27.16	36.40	51.15	79.79
$\nu_8(A_1)$	122.29	121.92	121.34	120.25	117.71	109.55
S_3 ν(RhCl)	14.44	14.84	15.71	17.14	19.13	14.32
S_4 ν(RhRh)	3.42	4.65	6.97	12.30	28.83	77.19
$S_8+S_9+S_{10}+S_{11}$	81.88	80.03	76.86	69.80	50.79	6.19
$\nu_{25}(B_2)$	220.58	220.58	220.58	220.58	220.58	220.58
S_{28} ν(RhCl)	94.51	94.51	94.51	94.51	94.51	94.51

The results of the NCA and PED calculations, as well as the band assignments (Table 4) are consistent with the data reported recently by Miskowski et.al. (ref. 18). The force constants for $[Rh_2X_2(OOCR)_2(N{-}N)_2]$ are consistent with a new comprehensive relationship between force constants and bond distances (ref. 18).

TABLE 4. The comparison between the calculated and observed wavenumbers for vibration of the X-Rh-Rh-X skeleton.

Complex	Force constants in mdyne A^{-1}		The calculated wavenumbers			The lines observed near the calculated values		
	K_{RhRh}	K_{RhCl}	$\nu_{3/4}(A_1)$	$\nu_{6/7}(A_1)$	$\nu_{25}(B_2)$	$\nu_{3/4}$	$\nu_{6/7}$	ν_{25}
1 · $4H_2O$	1.62	0.65	281	176.5	220.6	281,282	166,180	214,232
2	1.69	0.65	284	177	220.6	278,286	166,179	202,235
7 · $2H_2O$	1.68	0.65	283	178	220.6	276,288	168,180	210,225
10 · $2H_2O$	1.55	0.65	278.7	175	220.6	275,280	170,182	209,225
13 · $4H_2O$	1.60	0.65	279.5	176	220.6	276,284	168,180	220,237

APPLICATIONS

Rhodium(II) complexes of the $Rh_2(OOCR)_4$ type exhibit high catalytic activity in many reactions. One of the first recognized was the olefin hydrogenation catalyzed by $Rh_2(OAc)_4$ in strongly polar solvent. A mechanism involving heterolytic cleavage of dihydrogen has been proposed (ref. 33).

$$[Rh_2(OOCMe)_4] + H_2 \underset{k_{-1}}{\overset{k_1}{\rightleftharpoons}} [Rh_2H(OOCMe)_3] + H^+ + MeCOO^- \qquad (2)$$

$$[Rh_2H(OOCMe)_3] + \text{olefin} \xrightarrow{k_2} [Rh_2H(OOCMe)_3\text{olefin}] \qquad (3)$$

$$[Rh_2(OOCMe)_4] + \text{paraffin} \xleftarrow{H^+ + MeCOO^-} [Rh_2(\text{alkyl})(OOCMe)_3]$$

The complex 2 also catalyzed the olefin hydrogenation (ref. 5), although it is a less powerful catalyst as compared with rhodium(II) acetate. $Rh_2(OOCMe)_4$ in ethanol slowly catalyzes the alkene hydrogenation. More active catalysts were obtained in the basic ethanol solution (ref. 34). The highest hydrogenation rate was achieved using LiH as a base. Olefin reduction rate increases significantly after some induction time, when the rhodium acetate suffers decomposition. This was evidenced by electronic spectra of the reaction solutions, which indicated a distinct acceleration of the reduction at the moment of decay of the band at 17000 cm^{-1}, that is at the moment of decomposition of the rhodium(II) acetate. The reaction of a base with the rhodium(II) compound is accompanied by the break of acetate bridges, which allows the dissociation of a dimer to monomers and the reduction of rhodium(II) to rhodium(I). In the alkaline medium the hydrogenation is most likely catalyzed by the acetatoethanolato rhodium(I) complexes, which activate both hydrogen and olefin. Our ESR attempts to prove the presence of monomeric rhodium(II) complexes and of Rh(II)Rh(I) dimers failed. The formation of the latter could have been expected, because $RH_2(OOCR)_4$ complexes, as it was evidenced above (ref. 26,31) undergo the monoelectron electrochemical and radiolytical reduction. The hydrogen reduction of $Rh_2(OAc)_4$ would not proceed until substitution of acetate ligands by $C_2H_5O^-$. The measurements of electronic and ESR spectra revealed, that the monomeric rhodium(II) complexes and Rh(II)Rh(I) dimers, most likely intermediates undergo very fast disproportionation or reduction. $Rh_2(OOCR)_4$ carboxylates (R=H, Me, CH(OH)Ph) catalyze also the hydrogenation of olefins and ketones in basic alcohol solutions (in methanol, ethanol and isopropanol) in the presence of 2,2'-bipyridine and 1,10-phenanthroline and its derivatives as ligands. Measurements of ESR spectra of rhodium(II) acetate solution in the presence of 2,2'-bipyridine revealed the formation of Rh(II)Rh(I) intermediate complexes. The g values of 2.185 and 2.23 are similar to those for complexes obtained by radiolysis of 1 with ^{60}Co γ-rays. However in this case very broad signal with g=2.3 is also observed, suggesting that $[Rh_2(OAc)_4(bpy)_n]^-$ similar to 18 in DMF solution is formed. During the hydrogenation reaction appear intensive bands in electronic spectra in the range 9000 - 17000 cm^{-1}, indicative for the formation of the polynuclear rhodium(I) complexes (Table 5). Hydrogenation of olefins and ketones begins at the moment of the appearance of low energy bands in electronic spectra. This may suggest that catalytically active are polynuclear rhodium(I) complexes. The mechanism of formation of the catalytically active complexes could be written as follows (ref. 35).

$$[Rh_2(OAc)_4L_2] + 2\ bpy \longrightarrow [Rh_2(OAc)_4(bpy)_2] + 2L \quad (4)$$

$$[Rh_2(OAc)_4(bpy)_2] \xrightarrow{H_2} [Rh_2(OAc)_2(bpy)_2(solv)_2]^{2+} + 2\ OAc \quad (5)$$

$$[Rh_2(OAc)_4(bpy)_2] \xrightarrow{H_2} [Rh_2(OAc)_4(bpy)_2]^{-} \quad (6)$$

$$[Rh_2(OAc)_2(bpy)_2(solv)_2]^{2+} \xrightarrow{H_2} [Rh_2(OAc)_2(bpy)_2(solv)_2]^{+} \quad (7)$$

$$[Rh_2(OAc)_2(bpy)_2(solv)_2]^{+} \xrightarrow{H_2} [Rh_2(OAc)_2(bpy)_2] \quad (8)$$

$$[Rh_2(OAc)_4(bpy)_2]^{-} \xrightarrow{H_2} 2[Rh(OAc)(bpy)(solv)] + 2\ OAc^{-} \quad (9)$$

The catalyst formation rate depends upon the complex and ligand concentration and upon the nature of the latter. For pyridylphosphines $PPh_{3-x}(2\text{-}C_5\text{-}H_4N)_x$ (x = 1-3) the reduction proceeds without induction. The reduction rate of olefins and ketones depends on the nature of ligand and the ligand: Rh ratio. Competitive hydrogenation of olefins and ketones revealed that depending on L:Rh ratio either olefins or ketones could be reduced with high selectivity (Table 7). Most active catalysts for hydrogenation of ketones are $Rh_2Cl_2(OOCH)_2(bpy)_2$ and $Rh_2Cl_2(OOCH)_2(phen)_2$ (Table 6). The presence of bands in electronic spectra in the range 13000^2- 20000 cm^{-1} indicates, that also in this case the reduction could be catalyzed by polynuclear complexes (ref. 36)

TABLE 5. Electronic spectra of catalytic systems: 17 + 2bpy and 18 + 6bpy in 0.3 M NaOH methanolic solution.

Catalyst	Bands, μm^{-1} ($\varepsilon \cdot 10^{-2}$, $M^{-1}cm^{-1}$)*
17 + 2bpy	
after 30 min	0.95(2.45), 1.31(4.0), 1.71(8.6)
after 45 min	1.31(7.5), 1.80(14.7), 1.94(12.5)
after 60 min	0.84(6.3), 2.63(31)
18 + 6 bpy	
after 60 min	1.33(52), 1.54(70), 1.82(362), 1.92(292), 2.70(186)

|complex| = $5\ 10^{-4}$M

* The extintion coefficients were calculated assuming the formation of the of dimeric complexes.

TABLE 6. Catalysis of the hydrogenation of ketones by rhodium complexes in MeOH (0.3 M NaOH).

Catalyst	Maximum hydrogenation rate (mole H_2(mole Rh)$^{-1}$ h^{-1})			
	Me_2CO	cyclohexanone	$MeCOPr^i$	MeCOEt
1 + 4bpy	310	310	100	310
1 + 4phen	260	360	60	
2 + 4bpy	130			
16+ 4bpy	120			
17+ 4bpy	80			
1	30			
18+ 4bpy	130	160		100
18+ 6(2,9-di-Mephen)		200		

Volume of solution: $10cm^3$, 10^{-2} mole of ketone, $5 \cdot 10^{-6}$ mole of complexes, T = 303 K.

Table 7. Competitive hydrogenation of cyclohexene and cyclohexanone.

Catalyst	Products	$\frac{\text{cyclohexanol}}{\text{cyclohexane}}$ ratio
18 + 2bpy	cyclohexane,cyclohexanol	5.29
18 + 6bpy	cyclohexane,cyclohexanol	0.37
18 + 2(2,9-diMephen)	cyclohexane	0
18 + 6(2,9-diMephen)	cyclohexane	0

Solvent: 0.3 M NaOH in MeOH, T=303 K, 10^{-2}mole of cyclohexene, 10^{-2} mole cyclohexanone, $5 \cdot 10^{-6}$ mole of complex.

TABLE 8. Catalytic hydrogenation of cyclohexene by rhodium complexes.

Catalyst	Maximum hydrogenation rate of cyclohexene, mole H_2(mole Rh)$^{-1}h^{-1}$	Catalyst	Maximum hydrogenation rate of cyclohexene, mole H_2(mole Rh)$^{-1}h^{-1}$
17+2bpy	160	18+2L*	350
17+2phen	80	18+2quinine	140
17+2L	140	18+2apy	180
17+2L*	40	18+2PPh_3	800
17+2$P(py)_3$	0	18+2PPh_2py	600
18+2bpy	50	18+2$PPh(py)_2$	120
18+2phen	70	18+2$P(py)_3$	170
18+2L	0		

Solvent: 0.3 M NaOH in methanol, T = 303 K, 10^{-2} mole of cyclohexene, $5\cdot10^{-6}$ mole of complex, L = 4,7-diphenyl-1,10-phenathroline, L* = 2,9-dimethyl-1,10-phenathroline, apy = 2-aminopyridine.

The appearance of bands in the range 10000 - 20000 cm^{-1} was well documented for many square rhodium(I) complexes with Rh-Rh bond (ref. 38-40). Mestroni et.al. (ref. 13) have also assumed that the polynuclear dipyridyl and phenanthroline complexes acted as catalysts in contrary to the iridium catalysts, which are mononuclear $IIrX(C_6H_{10})(N\text{-}N)I$ (ref. 37). The complexes $Rh_2(OOCR)_4$ and $Rh_2Cl_2(OOCR)_2(bpy)_2$ in the presence of bpy catalyze the transfer hydrogenation of ketones using isopropanol in basic medium as donor. The reaction is rather fast; after 9 hrs more than 90% acetophenone was reduced. None of the 1-phenylethanol enantiomers was in excess for R = (S)-CH(OH)Ph although the catalyst activity depends on the nature of the carboxylato ligand.

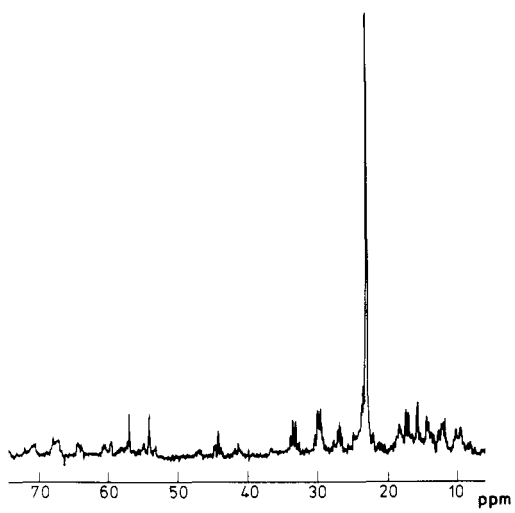

Fig. 3 ^{31}P NMR spectrum of catalyst formed in the reaction $Rh_2(OAc)_4$ + $P(2\text{-}C_5H_4N)_3$ in 70% EtOH (external reference: PPh_3 in $(CD_3)_2CO$).

The rhodium acetate forms in reaction with $P(2\text{-}C_5H_4N)_3$ (Rh:L = 1:1) in water alcohol solutions unusually active catalysts for the water gas shift reaction. They catalyze this reaction at low temperatures (70°C), with high rates (TN ~ 3 mole H_2(mole Rh)$^{-1}h^{-1}$. The ^{31}P NMR spectrum (Fig. 3) indicated the catalytic activity of the square and trigonal bipyramidal rhodium(I) complexes with rhodium: phosphine ratio equal to 1:1 and 1:2. Phosphine is coordinated with rhodium as a monodentate ligand via phosphorus atom and as a chelate ligand via P and N atoms. The following reaction mechanism was postulated:

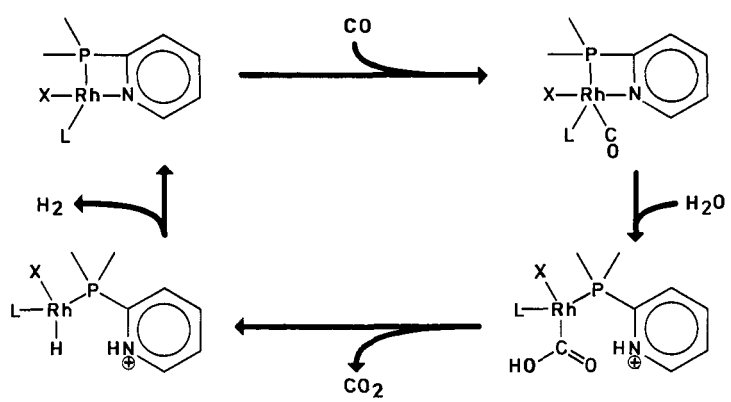

(10)

The cytostatic activity of the rhodium(II) carboxylate complexes was tested against KB cell line in vitro. The test was performed according to recommended international protocol for screening of chemical agents against tissue culture The complexes $[Rh_2(OOCCH(OH)Ph)_2(phen)_2(H_2O)_2](OOCCH(OH)Ph)_2$, $[Rh_2(OOCCH(OH)Me)_4(H_2O)_2]$, $[Rh_2(OAc)_2(phen)_2(H_2O)_2](OAc)_2$, $[Rh_2(OAc)_2(bpy)_2(H_2O)_2](OAc)_2$ revealed cytostatic activity higher or comparable with $Rh_2(OAc)_4$ which was used as a standard compound.

REFERENCES

1. F.A. Cotton, R.A. Walton, Multiple Bonds Between Metal Atoms, Wiley-Interscience, New York (1982), F.A. Cotton, R.A. Walton, Structure and Bonding, 62, 1 (1985).
2. E.B. Boyar, S.D. Robinson, Coord. Chem. Rev., 50, 109 (1983).
3. T.R. Felthouse, Progr. Inorg. Chem., 29, 73 (1982).
4. I.B. Baranovskii, M.A. Golubnichaya, L.M. Dikareva, R.H. Shchelokov, Zh. Neorg. Khim.,29, 1520 (1984); I.B. Baranovski, M.A. Golubnichaya, A.N. Zhilaev, R.N. Shchelokov, Koord. Khim., 13, 656 (1987).
5. H. Pasternak, F. Pruchnik, Inorg. Nucl. Chem. Letters, 12, 591 (1976).
6. F. Pruchnik, M. Zuber, Roczniki Chemii, 51, 1813 (1977).
7. F. Pruchnik, M, Zuber, H. Pasternak, K. Wajda, Spectrochim. Acta, 34A,1111 (1978).
8. F. Pruchnik, B.R. James, P. Kvintovics, Can. J, Chem, 64,936 (1986).
9. T. Głowiak, H. Pasternak. F. Pruchnik, Acta Cryst., C43, 1036 (1987).
10. A. Szymaszek, F. Pruchnik, Inorg. Chim. Acta, 131, 143 (1987).
11. F. Maspero, H. Taube, J. Am. Chem. Soc., 90, 7361 (1968).
12. J. Halpern, E. Kimura, J. Molin-Case, C.S. Wong, J. Chem. Soc. Chem. Commun., 1207 (1971).
13. M. Calligaris, L. Campana, G. Mestroni, M. Tornatore, E. Alessio, Inorg. Chim. Acta, 127, 103 (1987).
14. L. Dubicki, R.L. Martin, Inorg. Chem., 9, 673 (1970).
15. J.G. Norman, Jr. H.J. Kolari, J. Am. Chem. Soc., 100, 791 (1978); ibid., 101, 5256 (1979).
16. H. Nakatsuji, Y. Onishi, J. Ushio, T. Yonezawa, Inorg. Chem., 22, 1623 (1983)
17. P. Mougenot, J. Demyunck, M. Benard, Chem. Phys. Letters, 136, 279 (1987).
18. V.M. Miskowski, R.F. Dallinger, G.G. Christoph, D.E. Morris, G.H. Spies, W.H. Woodruff, Inorg. Chem., 26, 2127 (1987).
19. V.M. Miskowski, W.P. Schaeffer, B. Sadeghi, B.D. Santarsiero, H.B. Gray, Inorg. Chem., 23, 1154 (1984).
20. Yu. Ya. Kharitinov, G.Ya. Mazo, N.A. Knyazeva, Zh. Neorg. Khim., 15, 1440 (1970); I.K. Kireeva, G.Ya. Mazo, R.N. Shchelokov, ibid., 24, 396 (1979).
21. V.I. Sokol, M.A. Porai-Koshits, A.P. Kochetkova, L.B. Sveshnikova, Koord. Khim., 10, 844 (1984).
22. T. Głowiak, F. Pruchnik, B.R. James, unpublished results.
23. M.B. Hall, R.F. Fenske, Inorg. Chem., 11, 768 (1972).
24. L. Natkaniec, F. Pruchnik, submitted for publication.
25. L. Natkaniec, F. Pruchnik, in preparation.
26. F. Pruchnik, E. Kalecińska, A, Jezierski, submitted for publication.
27. G.W. Eastland, M.C.R. Symons, J. Chem. Soc. Dalton, 2193 (1984).
28. P. Piraino, G. Bruno, G. Tresoldi, S.Lo Schiavo, P. Zanello, Inorg. Chem., 26, 91 (1987); P. Piraino, G. Bruno, S.Lo Schiavo, F. Laschi, P. Zanello, ibid., 26, 2205 (1987).
29. A.R. Chakravarty, F.A. Cotton, D.A. Tocher, J.H. Tocher, Organometallics 4, 8 (1985).
30. M.Y. Chavan, T.P. Zhu, X.Q. Lin, M.Q. Ahsan, J.L. Bear, K.M. Kadish, Inorg. Chem., 23, 4538 (1984).
31. A. Szymaszek, F. Pruchnik, in preparation.
32. F. Pruchnik, J. Hanuza, K. Hermanowicz, K. Wajda-Hermanowicz, H. Pasternak, M. Zuber, submitted for publication.
33. B.C.Y. Hui, W.K. Teo, G.L. Rempel, Inorg. Chem., 12, 757 (1973).
34. M. Zuber, F. Pruchnik, Roczniki Chemii, 49, 1375 (1975).
35. H. Pasternak, F. Pruchnik, K. Wajda-Hermanowicz, M. Zuber, Polish J. Chem. in press.
36. H. Pasternak, E. Lancman, F. Pruchnik, J. Mol. Catal., 29, 13 (1985).
37. F. Vinzi, G. Zassinovich, G. Mestroni, J. Mol. Catal., 18, 359 (1983)
38. K.R. Mann, J.G. Gordon II, H.B. Gray, J. Am. Chem. Soc., 97, 3553 (1975).
39. V.M. Miskowski, I.S. Sigal, K.R. Mann, H.B. Gray, S.J. Milder, G.S. Hammond, P.R. Ryason, J. Am. Chem. Soc., 101, 4383 (1979).
40. A.L. Balch, J. Am. Chem. Soc., 98, 8049 (1976).
41. D. Duś, F. Pruchnik, in preparation.